Chemical Science

Accepted Manuscript

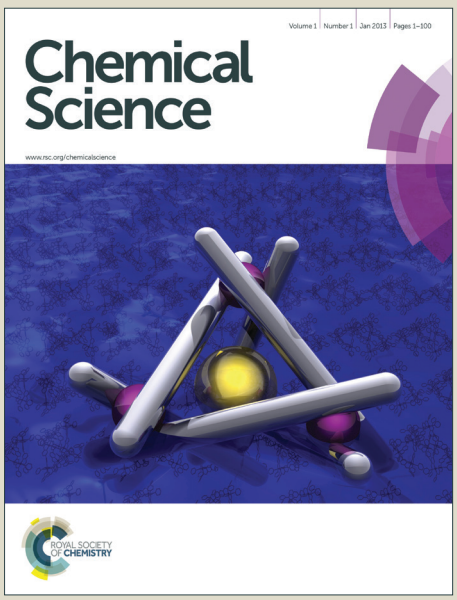

This is an *Accepted Manuscript*, which has been through the Royal Society of Chemistry peer review process and has been accepted for publication.

Accepted Manuscripts are published online shortly after acceptance, before technical editing, formatting and proof reading. Using this free service, authors can make their results available to the community, in citable form, before we publish the edited article. We will replace this *Accepted Manuscript* with the edited and formatted *Advance Article* as soon as it is available.

You can find more information about *Accepted Manuscripts* in the Information for Authors.

Please note that technical editing may introduce minor changes to the text and/or graphics, which may alter content. The journal's standard Terms & Conditions and the Ethical guidelines still apply. In no event shall the Royal Society of Chemistry be held responsible for any errors or omissions in this *Accepted Manuscript* or any consequences arising from the use of any information it contains.

ROYAL SOCIETY OF CHEMISTRY

www.rsc.org/chemicalscience

Chemical Science

RSCPublishing

EDGE ARTICLE

Multiplexed DNA Detection Based on Positional Encoding/Decoding with Self-Assembled DNA Nanostructures

Cite this: DOI: 10.1039/x0xx00000x

Received 00th January 2012,
Accepted 00th January 2012

DOI: 10.1039/x0xx00000x

www.rsc.org/

Sha Sun, Huaxin Yao, Feifei Zhang and Jin Zhu*

Current multiplexed analysis methods suffer from either slow reaction kinetics (planar arrays) or complicated encoding/decoding procedures (suspension arrays). We report herein a multiplexed DNA detection strategy that addresses these issues, based on positional encoding/decoding with self-assembled DNA nanostructures. The strategy enables the acquirement of high-resolution, consistent, and quantitative assay results in a single round of transmission electron microscopy imaging operation. Applications in polymerase chain reaction-free settings and assay of other structurally distinct targets can be anticipated through the implementation of the strategy with miniaturized femtoliter/attoliter dispensing technology and readily accessible DNA conjugate structures.

Introduction

The ability to detect multiple biologically relevant species in parallel allows the utilization of molecular profiling as an elaborate tool for the elucidation of biological phenomena. Such an information-intensive multiplexed analysis process has been enabled by two distinct assay formats, planar arrays[1] and suspension arrays.[2] Planar arrays provide convenient readout of targets through the positional encoding/decoding strategy, where the location of each spot in an ordered two-dimensional pattern defines the identity of a prospective target. This assay scheme is conceptually straightforward but suffers from slow reaction kinetics.[1d-1g] Suspension arrays exhibit fast reaction kinetics, but both of the encoding and decoding processes are generally rather complicated. An assay system that combines facile positional encoding/decoding capability and fast reaction kinetics would be ideal for efficient extraction of biological information.[3] Herein we report a multiplexed DNA detection strategy based on positional encoding/decoding with self-assembled DNA nanostructures (PED-SADNA) (Figure 1). Specifically, a self-assembled three-dimensional core DNA structure[4] with a registry marker asymmetrically positioned at one end and multiple types of target-binding capture probe sequences placed at regular intervals (collectively termed chip unit, or **CU**, by analogy to the planar DNA chip) is fabricated for the unambiguous positional encoding of DNA target information. Accordingly, multiple satellite DNA structures containing detection probe sequences (termed detection unit, or **DU**) for the remaining portions of corresponding targets are individually assembled. The presence of each target will direct the respective **DU** to the partner site of **CU** through hybridization. Staining of DNA nanostructures with uranyl formate and visualization with transmission electron microscopy (TEM) allow positional decoding and unambiguous identification of target DNA.

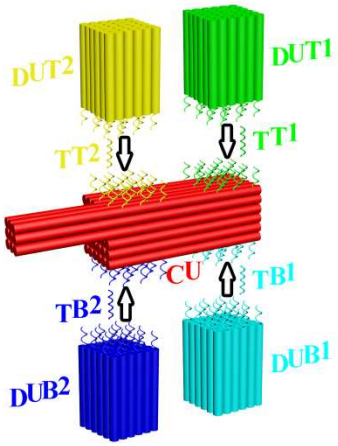

Figure 1. Schematic illustration of the PED-SADNA strategy. A **CU** is designed and assembled for the positional encoding, featuring a core cuboid with binding sites for multiple targets (**TT1**, **TT2**, **TB1**, **TB2**) and a registry marker at the corner as a reference for the differentiation of both lateral surfaces (top surface for **TT1** and **TT2**, bottom surface for **TB1** and **TB2**) and longitudinal positions (remote positions for **TT1** and **TB1**, proximal positions for **TT2** and **TB2**) where those sites are located. Accordingly, multiple **DU** (**DUT1**, **DUT2**, **DUB1**, **DUB2**) containing sequences that can hybridize with the remaining portions of corresponding targets are individually assembled. Target binding will direct the respective **DU** to the partner **CU** site. Staining with uranyl formate and TEM visualization allow positional decoding and unambiguous identification of target DNA.

Although self-assembled DNA nanostructures have been previously used for molecular diagnostics, they face major challenges with respect to the signal readout.[5,6] Atomic force

Chemical Science Accepted Manuscript

microscopy[5,7] allows high-resolution imaging down to the single-molecule level under optimized conditions, but the exact surface feature observed depends heavily on technical variables of a particular operation (e.g., expertise of operating personnel, morphology of scanning tip). Fluorescence microscopy[6,8] provides multi-color imaging capability, but limited spatial resolution and requirement for multiple imaging cycles/subsequent superposition processes (for the generation of pseudo-color images through multiple excitation source wavelengths or DNA strand exchange) poses significant restrictions on this sequential multiplexing methodology. The PED-SADNA method reported herein offers a robust solution to the above issues and delivers high-resolution, consistent, and quantitative assay results with a single round of TEM imaging operation.

Results and discussion

The asymmetric design of **CU** enables positional encoding at both lateral and longitudinal directions through the differentiation of surfaces and positions where the capture probes are located. The proof-of-concept **CU** system reported herein is comprised of a 6H (helices)/6H/128BP (base pairs) (all DNA sequences for self-assembly were designed with program Sequin[9] with a criton size of 7) square lattice core cuboid, which translates to a length scale of 15 nm/15 nm/43 nm, and a 3H/3H/64BP registry marker at a corner. The longitudinal dimension of the core cuboid and corner arrangement of the registry marker give a positional encoding capacity of four (two encoding positions for each surface × two surfaces). Accordingly, four types of capture probe sequences, each 11nt (nucleotides) in length and in 14 copies (with the end of core cuboid opposite to the registry marker counted as 0 BP, the locations of two capture probes are: 3 strands at 8 BP, 3 at 16 BP, 2 at 24 BP, 3 at 40 BP, 3 at 48 BP; and the locations of two other capture probes are: 3 at 88 BP, 3 at 104 BP, 2 at 112 BP, 3 at 120 BP, 3 at 128 BP) and specifically targeting a 26nt sequence, were integrated into the design of **CU** system. The gap distance between the two encoding sites on one surface is 13.5 nm, which can be readily resolved by TEM. For each of these targets, 15 copies of a 15nt detection probe sequence was engineered into a 6H/6H/64BP **DU** framework. Positional readout of **CU**-**DU** hybrid allows the extraction of target sequence information. In the **CU**/**DU** detection system reported herein, the location distributions of four target-binding sites in **CU** as described above secure a similar hybridization efficiency for each target. The size dimension of **CU** enables the docking of **CU**-**DU** hybrid in a desired side-on orientation on the TEM grid, which allows straightforward visualization of **DU**.

We commenced the evaluation of the feasibility of our detection system with a single-target (**TT1**) sample. This demands the fabrication and purification of corresponding **CU** and **DUT1**. These tailorable **CU** and **DU** can be conveniently synthesized by slow annealing of hundreds of single-strand DNA (ssDNA) sequences and subsequent purification with gel electrophoresis. A commonly observed phenomenon for self-assembled DNA nanostructures is undesired multimerization, especially after their extended storage at 4 °C. As such, before purification, a 4 h pre-heating step at 37 °C for the annealing product is needed for the increase of discrete cuboid recovery yield. Experiments with other alternative purification methods prove to be not as handy and effective as gel electrophoresis. Electro-elution[10] allows purification but involves extra solution exchange steps, and direct ultra-filtration[5a,11] can not completely eliminate excess ssDNA. In TEM imaging, instead of using glow discharge[12] for the creation of negative staining, we intentionally add a ssDNA sequence, which does not interfere with the assay, as a means of generating a hydrophilic TEM grid surface[13] for a convenient positive staining of **CU** and **DU**. Without assistance from such a ssDNA, limited access of aqueous solution due to the hydrophobicity of TEM grid results in only partial staining and damaged outlook for **CU** and **DU**. This positive staining method provides such high contrast for DNA nanostructures that we could image them easily in several minutes. With 5 nM each of purified **CU** and **DUT1** in hand and placed in the detection system, the presence of **TT1** (300 nM) leads to the formation of a lower mobility band in gel electrophoresis (Figure 2A) and TEM imaging confirmed the generation of **CU**-**DUT1** at the desired location (Figure 2B). Consistent with the expected existence of a size effect for the docking orientation of **CU** on TEM grid, an important experimental observation is that **CU** with a core cuboid size of

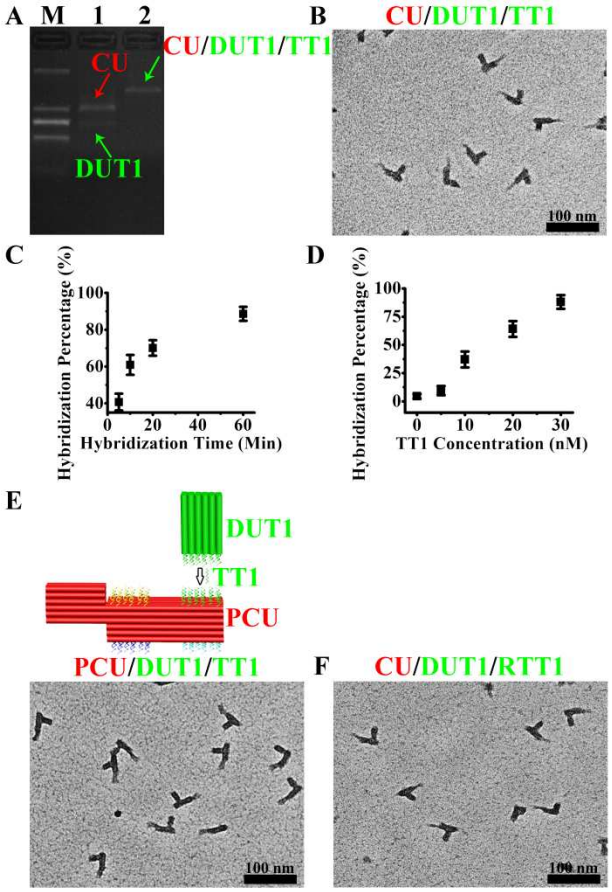

Figure 2. Single-target DNA and RNA detection with PED-SADNA. (A) Gel electrophoresis bands of **CU** and **DUT1** in the absence (lane 1) and presence (lane 2) of target DNA **TT1** (lane M represents molecular weight marker). (B) TEM image of **CU** and **DUT1** in the presence of target DNA **TT1**. (C) Hybridization percentage of **CU** and **DUT1** in the presence of target DNA **TT1** as a function of hybridization time. (D) Hybridization percentage of **CU** and **DUT1** in the presence of target DNA **TT1** as a function of concentration. (E) Schematic illustration and TEM image of **PCU** and **DUT1** in the presence of target DNA **TT1**. (F) TEM image of **CU** and **DUT1** in the presence of target RNA **RTT1**.

Chemical Science Accepted Manuscript

This journal is © The Royal Society of Chemistry 2012

6H/6H/128BP can achieve the desired side-on settlement, whereas a switch of its core cuboid to 6H/6H/64BP renders the majority of **CU** in head-on settlement, whether being alone or in the form of **CU**-**DU** hybrid. A screening of Mg^{2+} concentration indicates that hybridization proceeds efficiently at 11 mM. Statistical analysis by manual counting of each structurally resolved **CU** reveals a hybridization percentage (HP) of ~41% (defined as the percentage of observed **CU**-**DUT1** over all **CU**) after merely 5 min and ~89% (a plateau value comparable to that reported previously on DNA tiles[5a]) after 1 h (Figure 2C). Therefore, essentially, the whole assay can be accomplished within 74 min (1 h hybridization, 2 min loading of hybridization product onto TEM grid, 2 min staining, and 10 min TEM imaging). A longer duration of hybridization (8 h) provides essentially identical HP (~91%). Titration of **TT1** shows a positive correlation of HP with **TT1** concentration over the range of 10-30 nM, providing the possibility of target quantification (Figure 2D), and the HP of 30 nM (~89%) has reached the plateau value. It should be noted that **DUT1** can be occasionally identified at a location other than that targeted, as has also been observed previously in other self-assembled DNA systems.[6a] This "misplacement" of **DUT1**, due to either accidental proximal settlement of **CU** and **DUT1** on the TEM grid or non-specific interaction, can be counted as the background in our assay system. Indeed, such a phenomenon occurs even in the absence of a target DNA. The unoptimized detection limit therefore currently stands at 10 nM (HP ~37%, as compared with a background value of ~4%, Figure 2D). The ultimate measure of the assay sensitivity of a diagnostic method, in terms of absolute target quantity, is also dictated by the sample volume. In this regard, a major advantage of PED-SADNA strategy reported herein is the ability to scale down the sample volume without affecting the assay quality because of the high resolving power of TEM. When combined with the recently developed femtoliter/attoliter dispensing technology,[14] we anticipate that our detection system can be routinely applied in polymerase chain reaction (PCR, an amplification method that suffers from sensitivity to contamination and faces major issues in terms of multiplexing[15])-free settings. Overall, although both DNA self-assembly and TEM imaging seem, at first glance, inconvenient for the implementation of an assay tool, recent advances in both fields[4,16,17] with respect to automation and versatility render the PED-SADNA strategy demonstrated herein highly practical.

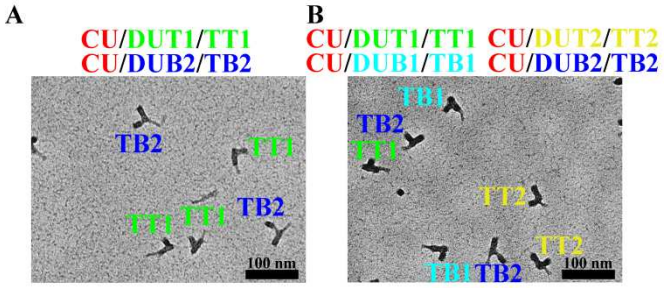

Figure 3. Two-target and four-target DNA detection with PED-SADNA. (A) TEM image of **CU**, **DUT1**, and **DUB2** in the presence of targets **TT1** and **TB2**. The hybridization was performed separately for **CU**/**DUT1** and **CU**/**DUB2**, followed by mixing the two solutions for TEM imaging. (B) TEM image of **CU**, **DUT1**, **DUT2**, **DUB1**, and **DUB2** in the presence of targets **TT1**, **TT2**, **TB1**, and **TB2**. The hybridization was performed separately for **CU**/**DUT1**, **CU**/**DUT2**, **CU**/**DUB1** and **CU**/**DUB2**, and then the hybridization solutions were combined into a single sample for TEM imaging.

The modular design of self-assembled DNA nanostructures allows the variation of registry marker to a protruded geometry (3H/6H/64BP) as an equally effective indicator of orientation for such a variant configuration, **PCU** (Figure 2E). Also, the **CU**/**DU** assay system can be adapted to the detection of other types of targets as long as corresponding target-binding probes are in place. RNA exists in a variety of forms and is an important diagnostic and therapeutic target. Indeed, the **CU**/**DUT1** design allows its direct application in the detection of a 26nt RNA target (**RTT1**) (Figure 2F).

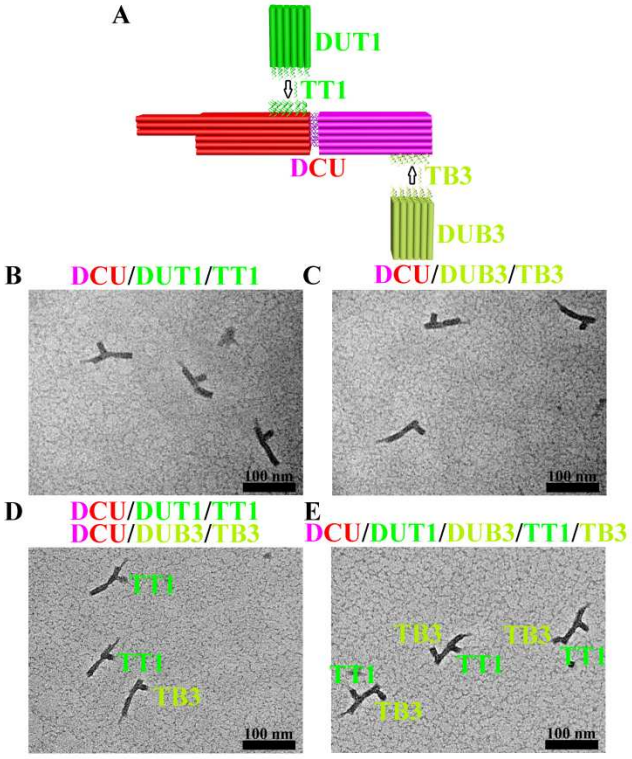

Figure 4. Expansion of positional encoding capacity through an increase of longitudinal dimension. (A) Schematic illustration of **DCU** design and two-target identification at discrete locations of both cuboids. (B) TEM image of **DCU** and **DUT1** in the presence of target DNA **TT1**. (C) TEM image of **DCU** and **DUB3** in the presence of target DNA **TB3**. (D) TEM image of **DCU**, **DUT1**, and **DUB3** in the presence of targets **TT1** and **TB3** (hybridization was performed separately for **DCU** and **DU** for each target and then the hybridization solutions were combined into a single sample for TEM imaging). (E) TEM image of **DCU**, **DUT1**, and **DUB3** in the presence of targets **TT1** and **TB3** (hybridization was performed simultaneously for **DCU** and **DU** for two targets and then the sample was subjected to TEM imaging).

With the single-target assay system validated, a two-target (**TT1**, **TB2**) sample was next examined. Accordingly, besides **CU** and **DUT1**, a second set of **DU** (**DUB2**) was fabricated and purified. The ability of **TB2** to bind **DUB2** to the target site of **CU** was then confirmed. For a two-target sample, the hybridization can be performed either separately with **CU**/**DUT1** and **CU**/**DUB2** (with a total ratio of **CU**/**DUT1**/**DUB2** approximately 2:1:1; mixing before TEM

Chemical Science Accepted Manuscript

imaging) or simultaneously with **CU**/**DUT1**/**DUB2** (with a ratio of approximately 1:1:1). As expected, separate hybridization gives discrete **CU**-**DUT1** and **CU**-**DUB2** hybrids whereas simultaneous hybridization enables the formation of **CU**-**DUT1**-**DUB2** hybrid. In either case, **DUT1** and **DUB2** hybridize orthogonally with **CU** in high efficiency only in response to the presence of corresponding targets, **TT1** and **TB2** (Figures 3A and S24), thus demonstrating the high selectivity of the assay system. Although the designed **CU** system allows for the encoding of four targets, multiplexed interrogation of four targets is a demanding assay scenario because of its contingency upon the elimination of cross-hybridization. Satisfactorily, with the fabrication of two additional sets of **DU** (**DUT2** and **DUB1**), four targets (**TT1**, **TT2**, **TB1**, **TB2**) can be unambiguously identified at the expected sites through high-yielding hybridization (Figures 3B and S29).

In principle, the positional encoding capacity is dictated by the longitudinal dimension of **CU** as well as the number of **CU** surfaces that can be distinguished (maximum four surfaces for a cuboid design with a properly configured registry marker). As a proof-of-concept demonstration of the ability to increase longitudinal dimension, a separate cuboid with an identical size to that of the core cuboid part of **CU** was fabricated and allowed to hybridize with **CU** to form a double-sized **DCU** (~86% yield at a Mg^{2+} concentration of 40 mM) (Figure 4A). As expected, **DCU** allows positional encoding at discrete locations of both cuboids (Figures 4B and 4C). A test with two-target (**TT1**, **TB3**) sample confirmed orthogonal hybridization and therefore effectiveness of this **DCU**/**DUT1**/**DUB3** system (Figure 4D). In addition, the large separation between the two encoding sites enables the better spatially resolved staining and imaging of both **DUT1** and **DUB3** on one **DCU** in the case of simultaneous hybridization (Figure 4E).

Conclusions

In summary, a multiplexed DNA detection strategy based on PED-SADNA has been developed. This strategy allows the simultaneous achievement of facile positional encoding/decoding and fast hybridization kinetics in a solution assay format. Miniaturized implementation in an ultra-small volume format should enable the routine application of the detection system demonstrated herein in PCR-free settings. Extension of the strategy to the assay of other structurally distinct targets is also foreseeable because of the synthetic availability of a large repertoire of DNA conjugates.

Acknowledgements

J.Z. gratefully acknowledges support from the National Natural Science Foundation of China (21274058) and the National Basic Research Program of China (2013CB922101, 2011CB935801).

Notes and references

[a] Department of Polymer Science and Engineering, School of Chemistry and Chemical Engineering, State Key Laboratory of Coordination Chemistry, Nanjing National Laboratory of Microstructures, Nanjing University, Nanjing 210093, China. Email: jinz@nju.edu.cn

† Electronic Supplementary Information (ESI) available: Experimental details, additional DNA detection figures, and DNA sequence information. See DOI: 10.1039/b000000x/

1 (a) *Microchip Methods in Diagnostics*, ed. U. Bilitewski, Humana Press, New York, 2009; (b) M. Debnath, G. B. K. S. Prasad and P. S. Bisen, *Molecular Diagnostics: Promises and Possibilities*, Springer, Dordrecht, 2010; (c) *Molecular Diagnostics: For the Clinical Laboratorian*, ed. W. B. Coleman and G. J. Tsongalis, Humana Press, New York, 2006; (d) M. Schena, D. Shalon, R. W. Davis and P. O. Brownt, *Science*, 1995, **270**, 467-470; (e) L. Shi, et al, *Nat. Biotechnol.*, 2006, **24**, 1151-1161; (f) R. D Canales, et al, *Nat. Biotechnol.*, 2006, **24**, 1115-1122; (g) M. J. Jonker, W. C. de Leeuw, M. Marinković, F. R. A. Wittink, H. Rauwerda, O. Bruning, W. A. Ensink, A. C. Fluit, C. H. Boel, M. de Jong and T. M. Breit, *Nucleic Acids Res.*, 2014, **42**, e94.

2 (a) J. Lee, P. W. Bisso, R. L. Srinivas, J. J. Kim, A. J. Swiston and P. S. Doyle, *Nat. Mater.*, 2014, **13**, 524-529; (b) D. C. Appleyard, S. C. Chapin, R. L. Srinivas and P. S. Doyle, *Nat. Protoc.*, 2011, **6**, 1761-1774; (c) H. Lee, J. Kim, H. Kim, J. Kim and S. Kwon, *Nat. Mater.*, 2010, **9**, 745-749; (d) D. C. Pregibon, M. Toner and P. S. Doyle, *Science*, 2007, **315**, 1393-1396; (e) K. Braeckmans, S. C. De Smedt, C. Roelant, M. Leblans, R. Pauwels and J. Demeester, *Nat. Mater.*, 2003, **2**, 169-173; (f) M. J. Dejneka, A. Streltsov, S. Pal, A. G. Frutos, C. L. Powell, K. Yost, P. K. Yuen, U. Müller and J. Lahiri, *Proc. Natl. Acad. Sci. USA*, 2003, **100**, 389-393; (g) S. R. Nicewarner-Peña, R. G. Freeman, B. D. Reiss, L. He, D. J. Peña, I. D. Walton, R. Cromer, C. D. Keating and M. J. Natan, *Science*, 2001, **294**, 137-141; (h) M. Han, X. Gao, J. Z. Su and S. Nie, *Nat. Biotechnol.*, 2001, **19**, 631-635; (i) S. Birtwell and H. Morgan, *Integr. Biol.*, 2009, **1**, 345-362.

3 (a) Y. Liu, H. Yao and J. Zhu, *J. Am. Chem. Soc.*, 2013, **135**, 16268-16271; (b) X. Shu, Y. Liu and J. Zhu, *Angew. Chem. Int. Ed.*, 2012, **51**, 11006-11009; (c) X. Zhou, S. Xia, Z. Lu, Y. Tian, Y. Yan and J. Zhu, *J. Am. Chem. Soc.*, 2010, **132**, 6932-6934; (d) X. Zhou, P. Cao, Y. Tian and J. Zhu, *J. Am. Chem. Soc.*, 2010, **132**, 4161-4168; (e) M. Hong, X. Zhou, Z. Lu and J. Zhu, *Angew. Chem. Int. Ed.*, 2009, **48**, 9503-9506; (f) F. Qiu, D. Jiang, Y. Ding, J. Zhu and L. L. Huang, *Angew. Chem. Int. Ed.*, 2008, **47**, 5009-5012.

4 (a) B. Wei, M. Dai and P. Yin, *Nature*, 2012, **485**, 623-627; (b) Y. Ke, L. L. Ong, W. M. Shih and P. Yin, *Science*, 2012, **338**, 1177-1183.

5 (a) Y. Ke, S. Lindsay, Y. Chang, Y. Liu and H. Yan, *Science*, 2008, **319,** 180-183; (b) Z. Zhang, Y. Wang, C. Fan, C. Li, Y. Li, L. Qian, Y. Fu, Y. Shi, J. Hu and L. He, *Adv. Mater.*, 2010, **22**, 2672-2675; (c) Z. Zhang, D. Zeng, H. Ma, G. Feng, J. Hu, L. He, C. Li and C. Fan, *Small*, 2010, **6**, 1854-1858; (d) H. K. K. Subramanian, B. Chakraborty, R. Sha and N. C. Seeman, *Nano. Lett.*, 2011, **11**, 910-913.

6 (a) C. Lin, R. Jungmann, A. M. Leifer, C. Li, D. Levner, G. M. Church, W. M. Shih and P. Yin, *Nat. Chem.*, 2012, **4**, 832-839; (b) R. Jungmann, M. S. Avendaño, J. B. Woehrstein, M. Dai, W. M. Shih and P. Yin, *Nat. Methods*, 2014, **11**, 313-318.

7 P. Eaton and P. West, *Atomic Force Microscopy*, Oxford University Press, Oxford, 2010.

8 (a) B. Huang, M. Bates and X. Zhuang, *Annu. Rev. Biochem.*, 2009, **78**, 993-1016; (b) M. Fernández-Suárez and A. Y. Ting, *Nat. Rev. Mol. Cell Biol.*, 2008, **9**, 929-943.

Chemical Science Accepted Manuscript

 This journal is © The Royal Society of Chemistry 2012

9 N. C. Seeman, *J. Biomol. Struct. Dyn.*, 1990, **8**, 573-581.
10 G. Bellot, M. A. McClintock, C. Lin and W. M. Shih, *Nat. Methods*, 2011, **8**, 192-194.
11 B. Ding, Z. Deng, H. Yan, S. Cabrini, R. N. Zuckermann and J. Bokor, *J. Am. Chem. Soc.*, 2010, **132**, 3248–3249.
12 C.-T. Bock, S. Franz, H. Zentgraf and J. Sommerville, Electron Microscopy of Biomolecules, in *Encyclopedia of Molecular Cell Biology and Molecular Medicine*, ed. R. A. Meyers, John Wiley & Sons, New York, 2006, pp. 103-128.
13 (a) M. Zheng, A. Jagota, E. D. Semke, B. A. Diner, R. S. Mclean, S. R. Lustig, R. E. Richardson and N. G. Tassi, *Nat. Mater.*, 2003, **2**, 338-342; (b) J. Robertson and E. P. O'Reilly, *Phys. Rev. B*, 1987, **35**, 2946-2957.
14 (a) S.-Y. Teh, R. Lin, L.-H. Hung and A. P. Lee, *Lab Chip*, 2008, **8**, 198–220; (b) P. W. Sutter and E. A. Sutter, *Nat. Mater.*, 2007, **6**, 363-366; (c) B. Qian, M. Loureiro, D. A. Gagnon, A. Tripathi and K. S. Breuer, *Phys. Rev. Lett.*, 2009, **102**, 164502; (d) A. Meister, M. Liley, J. Brugger, R. Pugin and H. Heinzelmann, *Appl. Phys. Lett.*, 2004, **85**, 6260-6262; (e) P. Actis, A. C. Mak and N. Pourmand, *Bioanal. Rev.*, 2010, **1**, 177-185; (f) T. Takami, B. H. Park and T. Kawai, *Nano Convergence*, 2014, **1**, 17.
15 N. L. Rosi and C. A. Mirkin, *Chem. Rev.*, 2005, **105**, 1547-1562.
16 (a) E. S. Andersen, M. Dong, M. M. Nielsen, K. Jahn, R. Subramani, W. Mamdouh, M. M. Golas, B. Sander, H. Stark, L. P. Oliveira, J. S. Pedersen, V. Birkedal, F. Besenbacher, K. V. Gothelf and J. Kjems, *Nature*, 2009, **459**, 73-77; (b) S. M. Douglas, H. Dietz, B. Liedl, F. Graf and W. M. Shih, *Nature*, 2009, **459**, 414-418; (c) D. Yan, S. Pal, J. Nangreave, Z. Deng, Y. Liu and H. Yan, *Science*, 2011, **332**, 342-346.
17 (a) J. B. Wagner, F. Cavalca, C. D. Damsgaard, L. D. L. Duchstein and T. W. Hansen, *Micron*, 2012, **43**, 1169-1175; (b) J. R. Jinschek, *Chem. Commun.*, 2014, **50**, 2696-2706; (c) F. Tao and M. Salmeron, *Science*, 2011, **331**, 171-174.

Chemical Science Accepted Manuscript